Pharm Res (2013) 30:1597–1607
DOI 10.1007/s11095-013-0998-3

RESEARCH PAPER

Microfluidic Synthesis of PEG- and Folate-Conjugated Liposomes for One-Step Formation of Targeted Stealth Nanocarriers

Renee R. Hood • Chenren Shao • Donna M. Omiatek • Wyatt N. Vreeland • Don L. DeVoe

Received: 23 October 2012 / Accepted: 28 January 2013 / Published online: 6 February 2013

ABSTRACT

Purpose A microfluidic hydrodynamic flow focusing technique enabling the formation of small and nearly monodisperse liposomes is investigated for continuous-flow synthesis of poly (ethylene glycol) (PEG)-modified and PEG-folate-functionalized liposomes for targeted drug delivery.

Methods Controlled laminar flow in thermoplastic microfluidic devices facilitated liposome self-assembly from initial lipid compositions including lipid/cholesterol mixtures containing PEG-lipid and folate-PEG-lipid conjugates. Relationships among flow conditions, lipid composition, and liposome size were evaluated; their impact on PEG and folate incorporation were determined through a combination of UV–vis absorbance measurements and characterization of liposome zeta potential.

Results PEG and folate were successfully incorporated into microfluidic-synthesized liposomes over the full range of liposome sizes studied. Efficiency of PEG-lipid incorporation was inversely correlated with liposome diameter. Folate-lipid was effectively integrated into liposomes at various flow conditions.

Conclusions Liposomes incorporating relatively large PEG-modified and folate-PEG-modified lipids were successfully synthesized using the microfluidic flow focusing platform, providing a simple, low cost, rapid method for preparing functionalized liposomes. Relationships between preparation conditions and PEG or folate-PEG functionalization have been elucidated, providing insight into the process and defining paths for optimization of the microfluidic method toward the formation of functionalized liposomes for pharmaceutical applications.

KEY WORDS microchannels · nanoparticles · nanotechnology · vesicles

ABBREVIATIONS

AF^4	asymmetric flow field-flow fractionation
Cryo-TEM	cryogenic temperature transmission electron microscopy
DCP	dihexadecyl phosphate
DMPC	1,2-dimyristoyl-sn-glycero-3-phosphocholine
DSPE-PEG_{2000}-folate	1,2-distearoyl-*sn*-glycero-3-phosphoethanolamine-N-[folate(PEG)-2000]
FPL	folate–PEG-modified liposomes
FR	folate receptor
FRR	flow rate ratio
FWHM	full width at half maximum
HEPES	4-(2-hydroxyethyl)-1-piperazineethanesulfonic acid
MALLS	multiangle laser light scattering
PEG	poly(ethylene glycol)
PEG_{2000}-PE	1,2-dimyristoyl-sn-glycero-3-phosphoethanolamine-N-[methoxy(PEG)-2000]
PEG_{5000}-PE	1,2-dimyristoyl-*sn*-glycero-3-phosphoethanolamine-N-[methoxy(PEG)-5000
PL	PEG-modified (PEGylated)
QELS	quasi-elastic light scattering

R. R. Hood • D. L. DeVoe
Fischell Department of Bioengineering
University of Maryland
College Park, Maryland 20742, USA

C. Shao • D. L. DeVoe
Department of Mechanical Engineering
University of Maryland
College Park, Maryland 20742, USA

R. R. Hood • D. M. Omiatek • W. N. Vreeland
Biochemical Sciences Division
National Institute of Standards and Technology
Gaithersburg, Maryland 20899-6313, USA

D. L. DeVoe (✉)
University of Maryland, 3139 Glenn L. Martin Hall, Building 088
College Park, Maryland 20742, USA
e-mail: ddev@umd.edu

INTRODUCTION

Liposomes are bilayer lipid vesicular nanoparticles that possess a range of highly attractive characteristics that make them excellent drug delivery vehicles; these characteristics include the ability to encapsulate aqueous solutions within the liposome core, sequester lipophilic compounds within the bilayer, and support tailored surface chemistries of the liposomes for targeted delivery. Liposome-encapsulated cancer therapeutics have been studied extensively and have shown to exhibit improved efficacies over non-encapsulated conventional drugs, by the former accumulating in their target sites due to the enhanced permeation and retention (EPR) effect present in tumor tissues, which permits liposomes to passively target cancerous tissue simply by leaking from the characteristically permeable hypervasculature and inadequate drainage present in tumors (1). Using this feature, liposomal anthracyclines (e.g., doxorubicin) have shown significantly reduced toxicity compared to conventional routes of administration for both adjuvant and metastatic breast cancer treatments, while exhibiting efficacies comparable to their traditional counterparts (2). These liposome-encapsulated compounds have also exhibited potent activity against a range of cancers including ovarian cancer and other solid tumors (3,4). Furthermore, "stealth" liposomes have been developed to provide further enhancement of this phenomenon by the addition of poly(ethylene glycol) (PEG) to the exterior surface as a flexible hydrophilic polymer to serve as a shield (5), inhibiting the binding of serum proteins (opsonins) which would otherwise activate an immune response and lead to rapid elimination of liposomes during circulation (4). Active targeting of liposomal drugs to the intended site may also be achieved by appending cell-specific ligands to the liposomes' exteriors, allowing the liposomes to efficiently and selectively dock with cells that overexpress high-affinity receptors for these ligands (6,7).

Despite ongoing advances in the development of targeted liposomal drugs, liposome preparation remains a cumbersome bulk-scale process based on classical methods including thin-film hydration, reverse-phase evaporation, rapid solvent exchange, or alcohol injection (8). Each of these bulk synthesis techniques requires laborious post-processing steps, such as serial membrane extrusion or sonication, to control the size and reduce the polydispersity of the resulting liposome population (8). Liposome size and size distribution are both crucial parameters for assuring controllable drug dosage, efficient cellular uptake, and extended *in vivo* circulation time. Smaller liposomes are known to exhibit slower blood clearance rates, and thus improved bioavailability (9,10). In addition to increasing the residence time of liposomes in the blood, smaller liposomes enhance the accumulation of nanoparticles within tumor cells, and also improve *in vivo* drug release (11). Perhaps more importantly, liposome size has a major impact on uptake by cancer cells, with both uptake rate and final internalized liposome concentrations enhanced as liposome radius is reduced (12). As a result, polydisperse liposome populations imply poorer safety profiles due to the need for larger amounts of drug to be administered to reach the desired therapeutic index. Moreover, the attachment of ligands such as PEG or targeting moieties to pre-formed liposomes can require additional processing steps for the post-insertion of functionalized lipids, further complicating established methods of liposomal drug preparation (13) and inevitably increasing the cost for development and manufacturing (14). Thus a key challenge is the realization of monodisperse formulations of targeted liposomal drugs, with controllable sizes below the limits defined by current bulk production methods, and supporting flexible protocols that may be optimized for specific liposome sizes, concentrations of encapsulated compounds, and functionalization of liposome membranes with targeting ligands.

The exquisite control over fluid flow conditions provided by microfluidics offers a unique path to liposome self-assembly through manipulation of interfacial interactions, particle diffusion, and convective-diffusive mixing of fluid phases. Using a simple microfluidic flow focusing technique which integrates the alcohol-injection method into a microfluidic device, nearly monodisperse populations of unilamellar liposomes with controllable sizes have been realized without the need for any post-processing steps to reduce size variance (15–17). Briefly, by this method, a center fluid stream of alcohol and solvated lipid is sheathed by two oblique streams of aqueous buffer *via* hydrodynamic focusing in a Y-channel microfluidic device (Fig. 1). Due to laminar flow resulting from low Reynolds numbers within the microfluidic system with channel dimensions on the order of several hundred microns, precise formation of nearly monodisperse populations of liposomes is achieved as a result of the controlled diffusive mixing which occurs at the interface of the two fluid streams.

Previous work on liposome production using the microfluidic flow focusing technique has concentrated on exploring the impact of changes in the ratio of volumetric flow rates between the buffer and alcohol streams on mean liposome size using a single native lipid species (15–17). In the present research, we explore microfluidic flow focusing as an effective method for continuous-flow preparation of nanoscale liposomes functionalized with PEG, enabling rapid and automated formation of stealth liposomes, and further extend the technique to the formation of liposomes functionalized with folate-PEG conjugates. Folate has been widely explored as a targeting moiety to selectively increase drug uptake by tissues overexpressing the folate receptor, a common theme among epithelial cancers and inflammatory

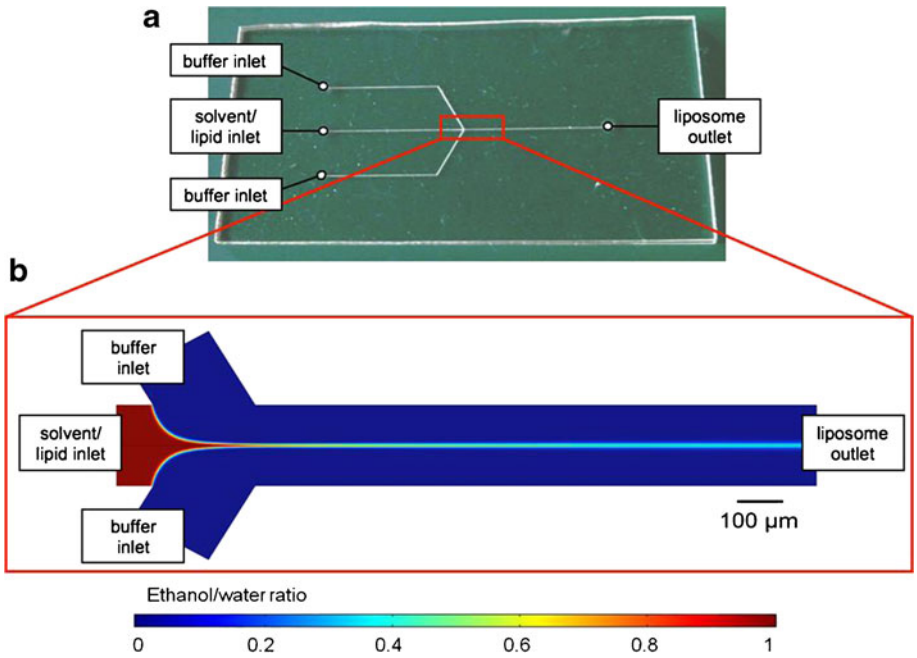

Fig. 1 (**a**) Photograph of the thermoplastic liposome synthesis chip, and (**b**) numerical simulation of hydrodynamic flow focusing in the microfluidic device, illustrating the diminishing mole fraction of ethanol along the center of channel as the alcohol (*red*) and aqueous buffer (*blue*) streams interact at a flow rate ratio of 70 within a 190 μm wide microchannel.

diseases (18,19). The resulting functionalized liposomes containing a combination of native lipids, PEG-lipids, and folate-PEG-lipids are characterized using a variety of analytical methods to explore the impact of microfluidic flow parameters on liposome size and surface properties. Asymmetric flow field-flow fractionation (AF^4) paired with multi-angle laser light scattering (MALLS) and quasi-electric light scattering (QELS) is used to evaluate size distributions of liposome populations formed under varying flow conditions and lipid compositions. To investigate the incorporation of the various lipid conjugates into the liposomes, UV-visible absorption spectroscopy, zeta potential measurements *via* phase analysis light scattering, and cryogenic temperature transmission electron microscopy are employed. Based on measurement results, the microfluidic platform is shown to provide a rapid, one-step method for preparing nearly monodisperse populations of folate receptor-targeted stealth liposomes of tunable size, with significant potential for drug delivery applications.

In addition to evaluating the microfluidic technology as a suitable method for on-line formation of functionalized liposomes, this work presents several ancillary advancements over previous studies. Unlike established efforts based on the use of silicon and glass microfluidic platforms, here we demonstrate the application of thermoplastic microfluidics as an alternative technology platform suitable for low-cost scale-up of the liposome synthesis technique. Furthermore, while prior studies have employed relatively toxic solvents such as isopropyl alcohol as a lipid carrier during microfluidic flow focusing (15–17), the present work utilizes ethanol as a less toxic solvent system to enhance biocompatibility for future *in vivo* applications.

MATERIALS AND METHODS

Certain commercial equipment, instruments, or materials are identified in this paper to foster understanding. Such identification does not imply recommendation or endorsement by the National Institute of Standards and Technology, nor does it imply that the materials or equipment identified are necessarily the best available for the purpose.

Device Fabrication

Microfluidic devices were fabricated in cyclic olefin copolymer (COC), a low-cost thermoplastic with excellent compatibility with a wide range of organic solvents, using a 2-step hot embossing process in which microfluidic channel features were first milled onto a polished Alloy 260 brass sheet (McMaster-Carr, Dayton, NJ) using a precision computer numerical control (CNC) milling machine (MDX-650A; Roland, Lake Forest, CA). The brass template was cleaned with a mild detergent, placed in a sonicator for 15 min, and examined under a microscope for imperfections. The brass template was then stacked in a commercial hot press (Carver, Wabash, IN) with a 48 mm thick polycarbonate plate (McMaster-Carr, Dayton, NJ) and held at a pressure of 0.8 MPa and temperature of 170°C for 5 min. The polycarbonate template with inverted channel features was then placed in the hot press with a 2 mm thick sheet of COC (Zeonor 1060 R, Zeon Chemicals L.P., Louisville, KY) and held at 0.4 MPa and 128°C for 10 min to transfer the pattern features from the PC intermediate template to the final COC chip. Using a LV-100 UDM microscope

(Nikon, Melville, NY) for optical profilometry, microchannel dimensions were found to be approximately 270 μm deep by 190 μm wide.

A cover plate with fluidic access ports was fabricated from a second 2 mm COC sheet using a CNC milling machine, and both COC pieces were degassed at 70°C under vacuum overnight. The chips were mated using solvent bonding with vapor-phase cyclohexane by placing the cover plate face down on top of a sealed glass beaker containing anhydrous cyclohexane (Sigma-Aldrich, St. Louis, MO) at 30°C, with the chip surface 5 cm away from exposed solvent, for 8.5 min. The chips were aligned and bonded in a hydraulic press (Carver, Wabash, IN) at 1.9 MPa for 1 min at room temperature. The bonded COC was held at room temperature for at least 24 h before use to maximize bonding strength. Press-fit needles were inserted at each fluidic access port and attached to nanoport fluidic connectors (Upchurch Scientific, Oak Harbor, WA) and silica capillary tubing (Polymicro Technologies Inc., Phoenix, AZ). The device was attached to glass gastight syringes (Hamilton Co., Reno, NV) containing buffer and lipid solution. Two programmable syringe pumps (Harvard Apparatus, Holliston, MA) were used for fluidic delivery and control.

Lipid Mixture and Hydration Buffer Preparation

For PEG-modified (PEGylated) liposomes (PL), 1,2-dimyristoyl-sn-glycero-3-phosphocholine (DMPC), cholesterol, and 1,2-dimyristoyl-*sn*-glycero-3-phosphoethanolamine-N-[methoxy(polyethylene glycol)-5000] (PEG_{5000}-PE) (all from Avanti Polar Lipids Inc., Alabaster, AL), and dihexadecyl phosphate (DCP) (Sigma-Aldrich, St. Louis, MO) were mixed in chloroform (Mallinckrodt Baker Inc., Phillipsburg, NJ) in the following proportions: DMPC/cholesterol/DCP/PEG_{5000}-PE in molar ratio (50-x)/40/10/x, where x=0, 5, 10, creating liposomes with 0 mol %, 5 mol %, and 10 mol % of PEG_{5000}-lipids. For folate-targeted PEGylated liposomes (FPL), DMPC, cholesterol, 1,2-dimyristoyl-sn-glycero-3-phosphoethanolamine-N-[methoxy(polyethylene glycol)-2000] (PEG_{2000}-PE), and 1,2-distearoyl-*sn*-glycero-3-phosphoethanolamine-N-[folate(polyethylene glycol)-2000] (DSPE-PEG_{2000}-Folate) (all from Avanti Polar Lipids Inc.), and DCP (Sigma-Aldrich) were mixed in chloroform (Mallinckrodt Baker) in the following proportions: DMPC/cholesterol/DCP/PEG_{2000}-PE/DSPE-PEG_{2000}-Folate in molar ratio 40-x/40/10/10/x, where x=0 or 2, as well as DMPC/cholesterol/DCP (50/40/10), creating PEGylated and folate-receptor targeted liposomes with 2 mol % DSPE-PEG_{2000}-Folate and both PEGylated and non-PEGylated liposomes as controls. The anionic surfactant DCP was included in all lipid preparations to prevent aggregation of liposomes in populations which did not contain PEG, as well as to assist in zeta potential measurements performed on all PLs. For PLs and FPLs, the lipid mixtures were prepared in scintillation vials then placed in a vacuum desiccator for at least 24 h to allow complete solvent removal. The dried lipid mixtures were then redissolved in anhydrous ethanol (99.5% Sigma-Aldrich) for a total lipid concentration of 20 mM. A 20 mM solution of 4-(2-hydroxyethyl)-1-piperazineethanesulfonic acid (HEPES) at pH 7.5 (Sigma-Aldrich) was used as an aqueous buffer in the microfluidic device. All solutions (solvent and buffer) were passed through 0.22 μm filters (Millipore Corp., New Bedford, MA) before being introduced to the microfluidic device.

Microfluidic Liposome Synthesis

Liposomes were prepared by injecting the lipid-solvent mixture between two buffer inputs into a microfluidic device, as done previously (16). HEPES buffer was injected into two oblique side channels intersecting with the center channel. The flow rate ratio (FRR), which is defined as the ratio of the volumetric flow rate of aqueous buffer to solvent, was set to 40, 70, and 100 for each PEG-lipid concentration to prepare PLs. The linear flow velocity of the combined fluid stream within the liposome formation channel was kept constant for all FRR values at 0.125 m/s, corresponding to a total volumetric flow rate of 384 μL/min. The hydrodynamic focusing region was observed with a TE-2000 S epifluorescence inverted microscope (Nikon, Melville, NY) throughout the liposome formation process to monitor for consistent flow conditions.

Asymmetric Flow Field-Flow Fractionation with Light Scattering and UV–vis Absorption Spectroscopy

High-resolution size-based separations of the liposome populations were carried out with AF^4. HEPES buffer was used as a carrier buffer for the separations. This was combined with MALLS, QELS, and UV–vis absorption for liposome detection and characterization (DAWN EOS and QELS, Wyatt Technology, Santa Barbara, CA). A vendor-supplied spacer (250 μm thickness) was used to define the flow channel thickness with a 10 kDa molecular weight cut-off regenerated cellulose membrane for the cross-flow partition (Millipore, Bedford, MA). The flow was controlled with Eclipse 2 software (Wyatt Technology, Santa Barbara, CA). A sample volume of 30 μL (all samples) was injected at a flow rate of 0.1 μL/min while focusing at 1.5 mL/min for 5 min. The injection step was succeeded by a second focusing step of 1.5 mL/min for 5 min. The crossflow was ramped linearly from 0.5 mL/min to 0 mL/min over a 30 min period while eluting the separated particles at 1 mL/min. The radii of the separated particles were measured using the MALLS and QELS detectors with data processing using ASTRA software (Wyatt Technology).

Static light scattering intensity (λ=690 nm) was measured at 15 angles simultaneously. The sample was analyzed at 1 s intervals by MALLS and 5 s intervals by QELS. The autocorrelation function of the QELS was fitted to a single-mode exponential decay model to resolve the hydrodynamic radii of the liposomes. A coated sphere model (i.e. a spherical structure with two radial regions of differing refractive index) of the MALLS data was consistent with this particle architecture and was used for size analysis of the geometric radius of the fractionated liposome samples. The ASTRA software generates information on the differential size distribution of each sample, which was used to analyze each population of liposomes. The differential distribution of each fractionated liposome sample produced a unimodal, sharp Gaussian distribution, indicating a nearly monodisperse population with a continuous size distribution. The modal diameter was taken to be the average diameter of each liposome population, in addition to the full width at half maximum (FWHM) to account for any polydispersity in the sample. In addition, UV–vis absorption spectroscopy was also used in-line to detect the presence of PEG on PLs (λ=520 nm) and folate on FPLs (λ=280 nm) in the fractionated samples.

Zeta Potential from Phase Analysis Light Scattering

The PL zeta potential was determined using phase analysis laser light scattering (ZetaPALS, Brookhaven Instruments Corp, Holtsville, NY) using undiluted PL samples (1.5 mL). All liposome mixtures used for zeta potential characterization contained 10 mol % DCP as an anionic surfactant, and were prepared in a low conductivity buffer (20 mM HEPES, conductivity ~60 μS). The incorporation of anionic DCP aided in electrophoretic measurements by providing the liposomes with a consistent surface charge density for each liposome sample. Electrophoretic motilities were measured and converted into zeta potentials using the Smoluchowski equation (20). Zeta potential measurements extrapolated from electrophoretic mobility measurements were averaged over 5 replicate runs of 10 cycles each. All measurements were carried out at 23°C.

Cryo-TEM Analysis

Aliquots from PL samples containing 0% and 10% PEG-lipid (FRR 40) were imaged using cryo-TEM. Sample preparation for cryo-TEM investigation was carried out using a Cryoplunge 3 unit (Gatan, Inc., Pleasanton, CA). A 3 μL volume of sample from 0%-PEG and 10%-PEG liposomes was pipetted onto a support grid held by tweezers directly above the cryoplunge workstation. The grid was aligned with the blot pads and was subsequently blotted for 4 s, giving a thin film between 100 nm-200 nm. The grid was then plummeted into liquid ethane in the workstation held at a temperature below −170°C with liquid nitrogen. This was repeated for both liposome samples and the grid was transferred to a cryo-holder for examination *via* transmission electron microscopy on a JEM 2100 LaB_6 TEM (JEOL, Japan).

RESULTS

Impact of PEG on Liposome Size and Distribution

MALLS and QELS in-line with AF^4 provided size information about the populations of liposomes produced by the microfluidic device. A single peak was present in each set of light scattering data obtained for all PL samples, indicating the presence of one primary species in the liposome samples with no aggregate formation (data not shown). The average geometric radii of the particles were determined by comparison against a coated sphere model (provided in the ASTRA software) and converted to diameters (Fig. 2). The modal diameter was taken as the average for each population (Fig. 3).

The size distributions of the liposomes followed the overall trends observed in former studies, which demonstrated that liposome size is influenced by the flow focusing conditions with size declining as the magnitude of flow focusing increases (i.e. higher FRRs) (15–17). The increased mismatch of fluid velocities between the alcohol and aqueous buffer flow streams as well as the narrower width of the alcohol flow stream, and therefore decreased diffusion lengths, observed at higher FRRs are thought to play a role in decreasing the size of the liposomes produced (21). Unlike these previous studies of liposome synthesis by microfluidic hydrodynamic focusing, which employed hybrid silicon/glass chips, the present work was performed using low-cost thermoplastic chips. It is notable that although the microchannel geometries, aspect ratios, roughness, precision, and surface properties all varied significantly from the previous silicon/glass chips, the devices were successful in producing size-tunable liposome populations with similarly low polydispersity as previous work, albeit with somewhat different relationships between flow rate ratio and mean liposome diameter.

Characterization of PEG Incorporation into PLs

The integration of PEG-lipids into PLs was first characterized through zeta potential measurements (Fig. 4). All PL samples exhibited a negative zeta potential due to DCP present in the liposomes, which decreased in absolute value as the PEG-lipid content of the liposomes increased. The absolute value of zeta potential remained relatively constant

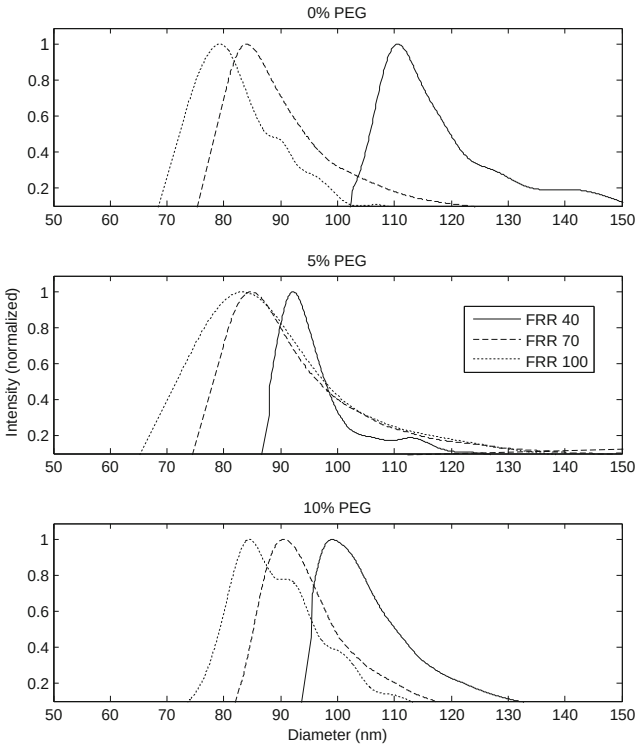

Fig. 2 Size distributions for liposomes composed of 0%, 5%, and 10% PEG-PE at each FRR. With increased flow focusing (higher FRR values), the diameters of the liposomes decrease in size. This trend is seen across all populations of liposomes, as well as the decrease in average size of liposome across the different lipid compositions at each FRR.

across the range of sizes produced, with the exception of the largest size formed at the lowest FRR for 10% PEG-PE.

Zeta potential represents the electrokinetic potential of the liposome at a distance from the outer membrane surface and expresses the degree of repulsion of adjacent particles from one another; it is a function of both particle surface charge and the nature of the surrounding environment including surface-bound ligands and thus is a useful tool for investigating the surface characteristics of PEGylated liposomes.

All liposome populations in this study contain equivalent concentrations of anionic DCP (10 mol %) and therefore have approximately equal negative net surface charge per unit area of membrane. However, the long, hydrophilic chains of PEG_{5000} serve as a shield to the liposome exterior, obstructing the negative surface charge provided by anionic DCP. Thus an increase of PEG molecules within the double layer will reduce the absolute value of the zeta potential due to the shielding effect of PEG on the negatively-charged liposome surface. Although a small amount of ethanol is present within each sample, the low mole fraction of ethanol in water at the various FRRs used does not result in significant changes in viscosity or dielectric constant (22), and thus does not appreciably alter liposome mobility.

Zeta potential measurements performed using microfluidic-synthesized liposomes convey successful integration of PEG-modified lipids into the liposomes. As revealed in Fig. 4, zeta potential is inversely correlated with PEG-PE concentration over the full range of liposome sizes studied here, confirming an increase in shielding of lipid charge resulting from higher surface density of PEG in the liposomes at higher PEG-PE concentrations. Overall, the decrease in the magnitude of zeta potential with increase in PEG-PE content provides strong confirmation that the PEG-lipid conjugates are successfully incorporated into the bilayer during the microfluidic flow focusing process.

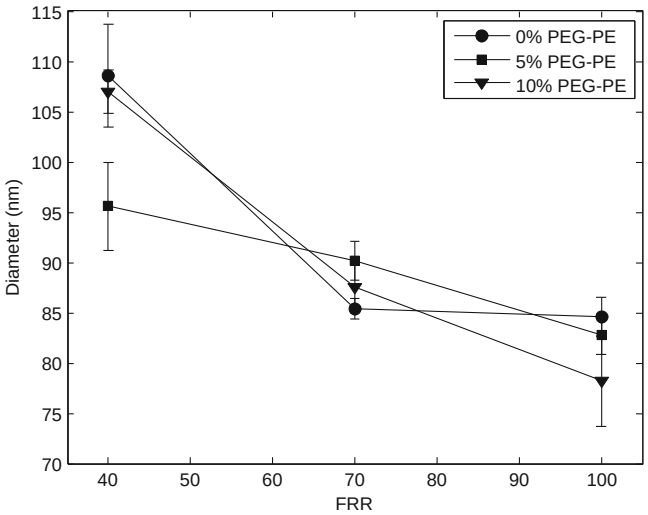

Fig. 3 Average geometric diameters of liposomes synthesized from lipid solutions with 0%, 5%, and 10% PEG-PE. Error bars are derived from the differential distribution of each liposome population, taken as the full width at half maximum divided by the modal diameter as seen in Fig. 2.

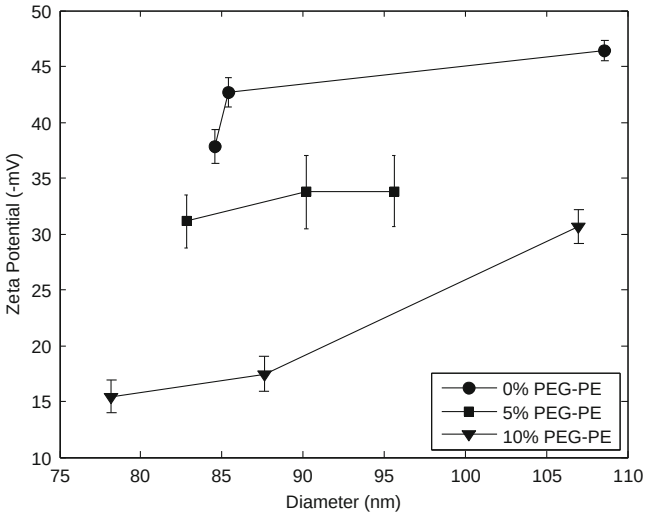

Fig. 4 Zeta potentials of 0%, 5%, and 10% PEG-PE liposomes. The absolute value of zeta potential decreased with increasing PEG-PE content at each given size, indicating the shielding effect of DCP, an anionic surfactant included in the liposomes, by the PEG molecules on the exterior of the liposomes.

Incorporation of PEG lipids into PLs was further evaluated using absorption spectroscopy measurements performed in-line with AF^4. Figure 5 depicts absorbance measurements over the same ranges of FRR and PEG_{5000}-PE concentration employed in the previous set of experiments. The presented data reflects the integrated absorbance at $\lambda = 520$ nm measured over a 3 min AF^4 elution time centered at the liposome elution peak to account for variations in liposome size distributions at each FRR. Note that the AF^4 fractionation ensures that any free PEG_{5000}-PE or PEG_{5000}-PE micelles within the microfluidic outflow do not contribute to the measurements in this test, which solely reflect the absorbance of the liposomes themselves. The integrated absorbance values presented in Fig. 5 are further normalized to the maximum level measured in this set of experiments.

Finally, PLs were analyzed with cryo-TEM imaging with 0 and 10 mol % PEG_{5000}-PE to verify liposome size and lamellarity. The cryo-TEM images of the 10% PEG liposomes did not reveal any form of micelles or aggregates, which supports the previous arguments that all PEG-lipids were incorporated into the liposomal membranes (Fig. 6).

Characterization of Folate Incorporation into FPLs

To evaluate the incorporation of folate-PEG lipids into FPLs, quantitative analysis of the concentration of folate in the liposomes was enabled by absorbance measurements taken at $\lambda = 280$ nm after being fractionated *via* AF^4. Using a molar extinction coefficient of ($\varepsilon = 25{,}280\ M^{-1}cm^{-1}$) (23), the concentration of folate was determined by UV–vis absorption measurements performed in-line with AF^4. A comparison of the measured folate content as a percentage of the hypothetical folate concentration calculated from the lipid mixture introduced for the given flow conditions is presented in Fig. 7. Absorbance values obtained for control liposomes were used as a baseline for all measurements to account for the absorbance caused by native lipid species. All of the resulting liposome populations, formed using a lipid mixture containing 2 mol % DSPE-PEG_{2000}-folate, showed a single peak of maximum absorbance coincident with the peak signal from light scattering, confirming that folate is only present in the liposome sample and is not eluted at a later time point as an aggregate. Folate content for FPLs was in general agreement with the calculated values. Additionally, a small signal was seen for PLs, indicating the presence of an additional species (PEG) on these vesicles (data not shown).

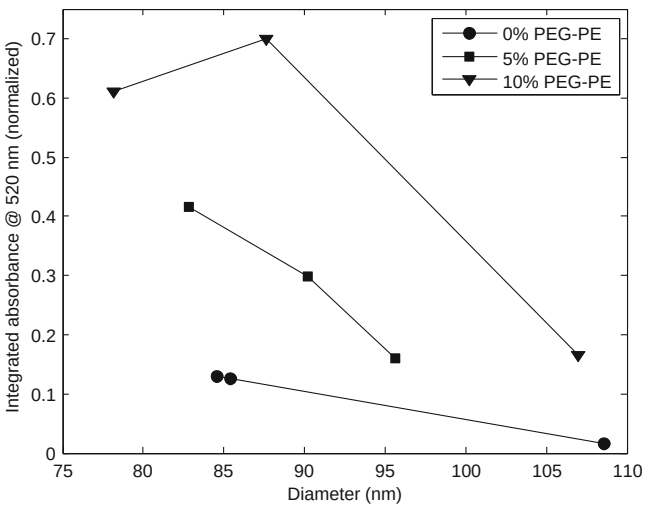

Fig. 5 Absorption measurements at $\lambda = 520$ nm performed in-line with AF^4 for 0%, 5%, and 10% PEG-PE liposomes. Each datum reflects the integrated absorbance intensity over a 3 min elution period centered on the liposome elution peak. Liposomes with 5% and 10% PEG-PE show significantly enhanced absorbance due to the presence of PEG on the liposomes.

DISCUSSION

Ongoing developments in the field of nanotechnology are enabling advances in drug delivery systems based on precisely engineered and functionalized nanoparticles. In particular, liposomes are a widely exploited class of nanoparticles due to their advantageous qualities and have played a noteworthy role in recent pharmacological advancements (24). Despite rapid growth in nanoparticle-enabled therapeutics, there remain significant limitations which must be addressed in order for nanoparticles to reach their full potential as pharmacological agents. Key challenges facing existing nanoparticle systems include restricted particle size control and reproducibility, high cost of production, challenging and costly methods for realizing tailored formulations, and indeterminate stability of the resulting therapeutic nanoparticles (25,26).

Nanoparticle behavior *in vivo* can vary drastically as a function of size, with significantly dissimilar pharmacokinetics and biodistribution resulting from small size variations (27). The synthesis of liposomes possessing well-defined sizes is particularly challenging, with conventional preparation methods commonly relying on poorly-controlled self-assembly of amphipathic constituents in turbulent flows, resulting in broad size distributions that require multiple post-processing steps to reduce polydispersity. This constraint increases both the time and cost of production, using processes that are further limited by the precision of the available materials used for the post-processing modification steps (e.g., size irregularity of nanometer-scale pores in polycarbonate membranes used for extrusion). The microfluidic method employed here enables controlled formation of liposomes by utilizing the intrinsic property of lipids to systematically self-assemble under laminar flow profiles which facilitate controlled diffusive mixing between miscible fluids and lipid species that exhibit differential solubility within the diffusing fluid streams. Microfluidic-directed formation of liposomes is a rapid process that produces liposomes with exceptionally low polydispersity,

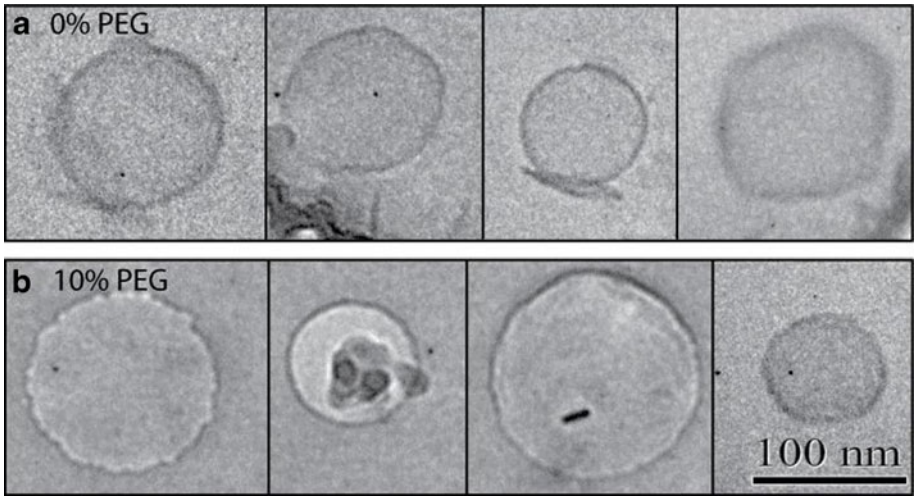

Fig. 6 Cryo-TEM images of liposomes formed using a lipid solution containing (**a**) 0% and (**b**) 10% PEG-lipid. Imaging results confirm the formation of unilamellar vesicles absent micelles or aggregates in both cases. Small ice crystals or artifacts that commonly form during vitrification, sample transfer, or elevation of specimen temperature due to the electron beam during cryo-TEM imaging seen in several images [28,29] do not reflect the presence of lipid aggregates.

with narrow size distributions significantly smaller than liposome populations obtained through conventional bulk-scale methods. At the same time, it is a single-step in-line process that eliminates the need for additional steps and equipment to be used for size homogenization. A central advance in the present work lies in application and characterization of the microfluidic technique toward the formation of functionalized liposomes, including the appendage of PEG and folate as a targeting ligand to the liposomal exterior, in a simple one-step process. Moreover, because the microfluidic technique eliminates the need for time consuming post-processing size homogenization and ligand insertion, liposomes may be rapidly prepared with custom formulations. This concept offers future potential for point-of-care applications, reducing the need for liposome preparations to maintain a prolonged shelf life. For example, liposomes with encapsulated enzymes and proteins have a limited shelf life, in some cases on the order of only hours or days, when simple electrostatic stabilization is employed (28). As a more aggressive future application of the technology, the microfluidic technique may also offer a path to on-demand synthesis of personalized drug formulations based on custom dosing, drug mixtures, or targeting ligands. The microfluidic technique is also shown to produce functionalized liposomes with tunable size and extremely narrow size distribution. It is expected that this feature will improve control over dosage while allowing more accurate prediction of the therapeutics' fate *in vivo*. In addition, the ability to synthesize narrow distributions of functionalized liposomes will enable unique pharmaceutical research opportunities, such as the investigation of pharmacokinetic and pharmacodynamic relationships across a range of liposome sizes which are nearly impossible to accurately assess using traditional methods.

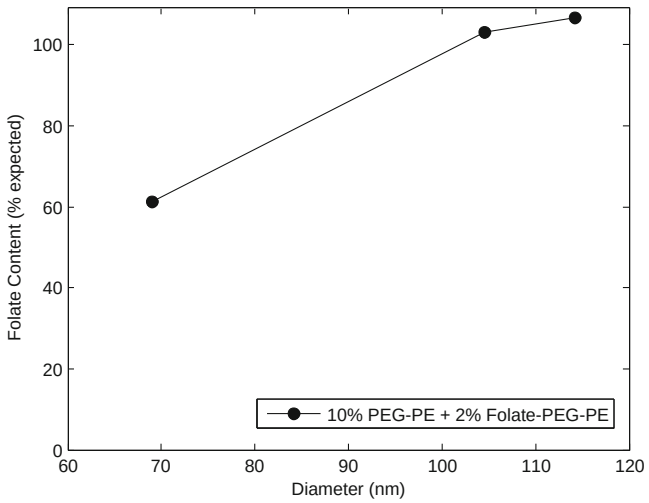

Fig. 7 UV–vis absorption data in line with AF[4] from folate (10% PEG-PE + 2% folate-PEG-PE) liposome samples, normalized to control (0% PEG-PE + 0% folate-PEG-PE) liposomes. Experimental values of liposome folate content are overall in agreement with theoretical values.

Here we demonstrate the ability to produce liposomes of tunable size with narrow size distributions, similar to previous studies (15–17), but within a low-cost thermoplastic microfluidic platform. Previous studies relied on microchannels created using costly materials (silicon or glass wafers and nanoports) as well as expensive, unnecessarily complicated fabrication techniques involving photolithographic patterning and high aspect ratio etching methods such as deep reactive ion etching. The present study abolishes the need for expensive materials and processes by exhibiting the ability to produce nearly-monodisperse liposomes in a continuous-flow process similar to previous studies within microchannels created in thermoplastic microfluidic chips *via* a two-step hot embossing technique, utilizing simple, inexpensive fabrication methods with much lower processing times. The transition from silicon to thermoplastic devices enables the microfluidic-directed liposome formation technique to be easily adopted in settings without cleanroom capabilities and significantly reduces the cost of device production. In addition, the use of inexpensive replication methods for microfluidic chip fabrication presents a realistic and cost-effective path toward parallelizing the

synthesis process, using multiple flow focusing chips acting in tandem for the rapid production of large volumes of liposomes.

Unlike previous work using isopropanol as a solvent for microfluidic-assisted liposome formation, here we have employed ethanol as a lipid carrier. The use of ethanol is significant for *in vivo* applications as its toxicity is significantly lower than that of other organic solvents, with a lethal blood level between 350 and 500 mg/dL, compared with 130–200 mg/dL for both methanol and isopropanol (29). While solvents other than ethanol may also be suitable for use with the microfluidic technique, each must be evaluated on an individual basis. For example, because chloroform is immiscible in water, the microfluidic method is not compatible with chloroform as a lipid carrier. Other carriers that are both miscible in water and compatible with the COC substrates used in this work, such as butanol, are likely to be feasible. However, the lateral distribution of solvent during flow focusing, and thus the point at which lipids self-assemble into leaflets and ultimately closed vesicles, is dependent on the nonlinear relationship between viscosity and solvent concentration across the diffusive water/solvent interface (17), and thus the size distributions of the resulting liposomes are expected to vary with solvent selection.

While prior work has focused on relationships between flow conditions and liposome size using native lipids, here we are interested in evaluating the impact on liposome size and size distribution by the addition of PEG_{5000}-lipid to the initial lipid mixture used in the microfluidic flow focusing process. The microfluidic device produced narrowly-distributed populations of liposomes with an overall decrease in liposome size with an increase in FRR, regardless of the presence of PEG-PE in the lipid mixture (Fig. 2). Liposomes formed in the absence of PEG were found to exhibit an inverse relationship between FRR and liposome diameter, as shown in Fig. 3. The error bars in this figure reflect the FWHM distribution of each liposome population. This figure also reveals a very similar behavior for PLs formed at both concentrations of PEG_{5000} explored in this study. The liposome populations produced by the microfluidic flow focusing method do not significantly change with PEG_{5000}-lipid concentration, but remain largely controlled by the flow conditions used in the focusing process. This is not necessarily an expected outcome considering the roles of hydrodynamics and diffusion in the liposome formation process (17). The average on-chip residence time in our studies was only 250 ms, and liposome formation likely occurs within an even shorter time during the initial mixing zone at the confluence of the lipid and aqueous streams. Given that PEG_{5000} is approximately eight times the molecular weight of the native lipids used in the initial mixture, differences in diffusive transport for the PEG-modified lipids as well as steric hindrance during the self-assembly process could be expected to affect the liposome formation process. The data presented in Figs. 2 and 3 reveals that the microfluidic process produces liposomes with consistent size under the given range of flow conditions despite the inclusion of PEG-modified lipids. Similarly, no significant variation in liposome size distribution is observed.

As revealed in Fig. 4, zeta potential was found to be directly correlated with liposome radius, with the strength of this correlation depending on PEG-PE concentration. This latter observation may result from reduced steric interactions between PEG chains for higher curvature vesicles (30), encouraging preferential incorporation of PEG-PE into smaller liposomes and concomitant increase in charge shielding. Additionally, the shielding effect PEG on the liposome is greater at 10 mol % PEG-PE than at 5 mol % PEG-PE. The greater degree of observed charge shielding at each liposome size for the 10 mol % PEG-PE liposomes may be due to the anticipated formation of a brush configuration at this high PEG concentration. Although further characterization is needed to verify this hypothesis, surface-grafted PEG molecules are known to prefer a tightly packed brush configuration resulting in extension of the linear PEG chains at high surface concentrations, while a more loosely arranged mushroom or transition regime occurs at lower concentrations (31). Overall, the inverse correlation between zeta potential and PEG-PE content reveals that the PEG-conjugated lipids are effectively incorporated into the liposomes using the microfluidic flow focusing process. The incorporation of PEG-lipids was further confirmed by UV–vis absorbance analysis (Fig. 5), with the resulting data consistent with the hypothesis that incorporation of PEG-PE lipids is favored during interactions with higher curvature membranes, and thus are more readily incorporated into smaller liposomes.

Cryo-TEM imaging was performed to ensure that the presence of large PEG molecules did not affect vesicle unilamellarity. The imaging results shown in Fig. 6 reveal a spherical morphology and overall agreement in size compared to the size information obtained from light scattering. PEGylated liposomes and control liposomes appear similar size and shape. While PEG cannot be directly imaged *via* electron microscopy without the addition of contrast surfactants due to insufficient electron density (32), the data confirms that unilamellar liposomes are formed in both cases, with an average membrane thickness of 5.4 ± 0.6 nm corresponding to the expected bilayer membrane thickness of DMPC in water (33). Lipid bilayer thickness was determined using the scale bar provided by the TEM instrument, with each reported value reflecting the average from 4 measurements performed on 4 individual liposomes.

Figure 7 shows the concentration of folate on FPLs from values obtained *via* the UV–vis absorption spectroscopy. The integrated values for folate are largely in agreement with the expected folate content, indicating successful inclusion of DSPE-PEG_{2000}-folate into the FPLs at approximately the same

molar ratio of folate-conjugated lipids in the initial lipid mixture. The larger FPLs with diameters above 100 nm, corresponding to FRRs of 40 and 70, exhibited folate concentrations slightly above the initial mixture concentration. While the measured folate concentration in the smaller FPLs was only 60% of the initial molar ratio, this may be due to the reduced liposome concentration associated with the high FRR value of 100 used to form these FPLs, resulting in absorbance signals near the detection limit of the UV–vis spectrometer. Thus, while all of the liposomes exhibited clear evidence of folate incorporation, the high level of uncertainty in the absorbance data for the smallest liposomes does not support a conclusion that the final concentration of folate is related to liposome size.

Application of the microfluidic technique to liposomal drug preparation will require scale-up of the technology for the production of large liposome volumes at concentrations suitable for *in vivo* use. Ultimately, we envision the use of a dense array of individual flow focusing elements fabricated on a single 10 cm square thermoplastic chip, with on-chip flow splitters used to control the delivery of solvent, buffers, and functional reagents to the parallel flow focusing channels. Of the parameters known to have a direct impact on liposome size, including channel geometry, temperature, and buffer ionic strength, liposome size is most sensitive to changes in FRR. Photolithographic control of the imprinting mold used for channel fabrication can ensure uniform hydrodynamic resistance across the microchannel array, and thus uniform flow rates and FRR values for precise and reliable control over liposome size during process scale-up.

CONCLUSION

This study demonstrates the successful extension of microfluidic-directed liposome formation technology to include the continuous, controlled synthesis of nearly monodisperse populations of PEG-modified and folate receptor-targeted liposomes. Liposomes comprised of DMPC and cholesterol with varying compositions of PEG_{5000}-lipids, PEG_{2000}-lipids, and folate-PEG_{2000} lipids have been successfully formed using a thermoplastic microfluidic chip enabling adjustable hydrodynamic focusing of a stream of lipids dissolved in an organic solvent by miscible streams of an aqueous buffer. Despite the large difference in molecular weight between the native lipids explored in previous studies and the PEG-lipid and folate-PEG-lipid conjugates used in this work, no significant difference in liposome size or size distribution was observed between these two cases. This technique opens doors for a variety of liposome applications, such as the ability to provide PEG-modified liposomes and folate-targeted liposomes with tunable characteristics and lipid compositions for targeted drug delivery. Further, the ability to achieve rapid, one-step synthesis of functionalized, unilamellar liposomes has great potential for further development toward the realization of on-chip liposome "microfactories" wherein liposome formation, liposome functionalization, and drug encapsulation is performed with real-time control over the resulting nanocapsule properties.

ACKNOWLEDGMENTS AND DISCLOSURES

Cryo-TEM imaging was performed at the Nanoscale Imaging, Spectroscopy, and Properties (NISP) Laboratory of the Maryland NanoCenter at the University of Maryland, College Park. This research was supported by NIH grants R21EB011750 and R21EB009485, NSF grant CBET0966407, NIST-ARRA Fellowship Program administered by the University of Maryland, and the NRC Research Associateship Program.

REFERENCES

1. Maeda H, Wu J, Sawa T, Matsumura Y, Hori K. Tumor vascular permeability and the EPR effect in macromolecular therapeutics: a review. J Control Release. 2000;65(1–2):271–84.
2. O'Shaughnessy J. Liposomal anthracyclines for breast cancer: overview. Oncologist. 2003;8 Suppl 2:1–2.
3. Patri AK, Majoros IJ, Baker JR. Dendritic polymer macromolecular carriers for drug delivery. Curr Opin Chem Biol. 2002;6(4):466–71.
4. Moghimi SM, Szebeni J. Stealth liposomes and long circulating nanoparticles: critical issues in pharmacokinetics, opsonization and protein-binding properties. Prog Lipid Res. 2003;42(6):463–78.
5. Immordino ML, Dosio F, Cattel L. Stealth liposomes: review of the basic science, rationale, and clinical applications, existing and potential. Int J Nanomedicine. 2006;1(3):297–315.
6. Forssen E, Willis M. Ligand-targeted liposomes. Adv Drug Deliv Rev. 1998;29(3):249–71.
7. Zhao X, Li H, Lee RJ. Targeted drug delivery *via* folate receptors. Expert Opin Drug Deliv. 2008;5(3):309–19.
8. Jesorka A, Orwar O. Liposomes: technologies and analytical applications. Annu Rev Anal Chem. 2008;1(1):801–32.
9. Ishida T, Harashima H, Kiwada H. Liposome clearance. Biosci Rep. 2002;22:197–224.
10. Litzinger DC, Buiting AM, Van Rooijen N, Huang L. Effect of liposome size on the circulation time and intraorgan distribution of amphipathic poly(ethylene glycol)-containing liposomes. Biochim Biophys Acta. 1994;1190:99–107.
11. Nagayasu, Uchiyama, Kiwada. The size of liposomes: a factor which affects their targeting efficiency to tumors and therapeutic activity of liposomal antitumor drugs. Adv Drug Deliv Rev. 1999;40(1–2):75–87.
12. Ramachandran S, Quist AP, Kumar S, Lal R. Cisplatin nanoliposomes for cancer therapy: AFM and fluorescence imaging of cisplatin encapsulation, stability, cellular uptake, and toxicity. Langmuir. 2006;22:8156–62.
13. Uster PS, Allen TM, Daniel BE, Mendez CJ, Newman MS, Zhu GZ. Insertion of poly(ethylene glycol) derivatized phospholipid into pre-formed liposomes results in prolonged *in vivo* circulation time. FEBS Lett. 1996;386(2–3):243–6.
14. Gu FX, Karnik R, Wang AZ, Alexis F, Levy-Nissenbaum E, Hong S, *et al.* Targeted nanoparticles for cancer therapy. Nano Today. 2007;2(3):14–21.

15. Jahn A, Vreeland WN, Gaitan M, Locascio LE. Controlled vesicle self-assembly in microfluidic channels with hydrodynamic focusing. J Am Chem Soc. 2004;126:2674–5.
16. Jahn A, Vreeland W, DeVoe DL, Locascio L, Gaitan M. Microfluidic directed self-assembly of liposomes of controlled size. Langmuir. 2007;23:6289–93.
17. Jahn A, Stavis SM, Hong JS, Vreeland WN, DeVoe DL, Gaitan M. Microfluidic mixing and the formation of nanoscale lipid vesicles. ACS Nano. 2010;4(4):2077–87.
18. Nakashima-Matsushita N, Homma T, Yu S, Matsuda T, Sunahara N, Nakamura T, *et al.* Selective expression of folate receptor beta and its possible role in methotrexate transport in synovial macrophages from patients with rheumatoid arthritis. Arthritis Rheum. 1999;42(8):1609–16.
19. Hansen MJ, Low PS. Folate receptor positive macrophages: cellular targets for imaging and therapy of inflammatory and autoimmune diseases. In: Jackman AL, Leamon CP, editors. New York, NY: Springer New York; 2011. p. 181–93.
20. Somasundaran P, editor. Encyclopedia of surface and colloid science, Second ed. Taylor & Francis; 2006.
21. Zook JM, Vreeland WN. Effects of temperature, acyl chain length, and flow-rate ratio on liposome formation and size in a microfluidic hydrodynamic focusing device. Soft Matter. 2010;6(6):1352.
22. Yilmaz H. Excess properties of alcohol—water systems at 298.15 K. Turk J Phys. 2002;26:243–6.
23. Mitchell HK. Folic acid. IV. Absorption spectra. J Am Chem Soc. 1944;66(2):274–8.
24. Torchilin VP. Recent advances with liposomes as pharmaceutical carriers. Nature reviews. Drug Discov. 2005;4(2):145–60.
25. Edwards KA, Baeumner AJ. Analysis of liposomes. Talanta. 2006;68(5):1432–41.
26. Couvreur P, Vauthier C. Nanotechnology: intelligent design to treat complex disease. Pharm Res. 2006;23(7):1417–50.
27. Gaumet M, Vargas A, Gurny R, Delie F. Nanoparticles for drug delivery: the need for precision in reporting particle size parameters. Eur J Pharm Biopharm Official Journal of Arbeitsgemeinschaft für Pharmazeutische Verfahrenstechnik eV. 2008;69(1):1–9.
28. Lasic DD. Liposomes: from physics to applications. Amsterdam; New York: Elsevier; 1993.
29. Rosano TG. Methanol and isopropanol toxicology with clinical applications [Internet]. Am Assoc Clin Chem. 2011. Available from: http://www.aacc.org/events/online_progs/Documents/Methanol-Isopropanol_revised.pdf.
30. Montesano G, Bartucci R, Belsito S, Marsh D, Sportelli L. Lipid membrane expansion and micelle formation by polymer-grafted lipids: scaling with polymer length studied by spin-label electron spin resonance. Biophys J. 2001;80(3):1372–83. Elsevier.
31. De Gennes PG. Conformations of polymers attached to an interface. Macromolecules. 1980;13(5):1069–75.
32. Almgren M, Edwards K, Karlsson G. Cryo transmission electron microscopy of liposomes and related structures. Colloids Surf, A Physicochem Eng Asp. 2000;174(1–2):3–21.
33. Nagle JF, Tristram-Nagle S. Structure of lipid bilayers. Biochim Biophys Acta Rev Biomembr. 2000;1469(3):159–95.